Original Article ISSN (Online): 2582-7472

PARTIAL SLIP EFFECT OF CU, AU, TIO2-NANO PARTICLE IN STUDY BIO MAGNETIC MAXWELL FLUID FLOW AND HEAT TRANSFER OVER A STRETCHING SHEET IN THA PRESENCE OF MAGNETIC DIPOLE

Channakeshava Murthy 1 , Manjunatha P T 2 , Lokesh T 2

- Associate Professor, Department of Mathematics, Government First Graed College, Bidar, Karnataka, India
- ² Associate professor, Department of Mathematics, Government Science College, Chitradruga, Karnataka, India





CorrespondingAuthor

Channakeshava Murthy. gurckm123@gmail.com

10.29121/shodhkosh.v3.i2.2022.260

Funding: This research received no specific grant from any funding agency in the public, commercial, or not-for-profit sectors.

Copyright: © 2022 The Author(s). This work is licensed under a Creative Commons Attribution International License.

With the license CC-BY, authors retain the copyright, allowing anyone to download, reuse, re-print, modify, distribute. and/or copy contribution. The work must be properly attributed to its author.



ABSTRACT

In this paper, we analyzed the Bio magnetic Maxwell fluid flow and heat transfer in a Nano fluid over a stretching sheet in the presence of magnetic dipole. The effects of velocity slip are considered in this study. Three different types of Nano fluids, namely the Copperblood, the Gold- blood and titanium dioxide-blood are considered. The governing partial differential equations are transformed into ordinary differential equations using suitable transformation. Numerical solutions of these equations are obtained by using maple software. Inside the boundary layer, the variations of velocity, temperature various values of the appearing parameter, namely the ferromagnetic parameter, viscous dissipation parameter, dimensionless distance, dimensionless curie temperature, Deborah number, slip parameter are presented graphically and discussed in detail. The obtained results show that Gold has higher rate of heat transfer compared to Copper and Titanium dioxide. A good agreement is found between the present numerical results and the available results in the literature in some specific cases.

Keywords: Communication, Circumstance, Elements, Organisational

1. INTRODUCTION

Due to the wide range of applications of biomagnetic fluid especially in the area of medical and bioengineering, it has gained a serious attention from the researcher since last decades. Biomagnetic fluid dynamics (BFD) analyzes the biological fluid under the effects of magnetic field. Bio magnetic fluid is present in a living creature. The most characteristic of bio magnetic fluid is blood. Blood is a non-Newtonian fluid which is made of plasma, red blood cells, white blood cells and others. The study on blood is of great significance due to its applications (10-50nm) in usual heat transfer fluids.

To study the flow of biomagnetic fluid ,the first BFD model was proposed by Haik et al [1], Effects of variable viscosity and thermal conductivity on MHD flow and heat transfer of a dusty fluid Manjunatha et al [2], Slip flow of a

Maxwell fluid past a stretching sheet. Walailak Journal of Science and Technology. Sajid et al [3], Impact of magnetic dipole on thermophoretic particle deposition in the flow of Maxwell fluid over a stretching sheet Naveen kumar et al [4], Numerical study of biomagnetic fluid flow in a duct with a constriction affected by a magnetic field Mousavi et al [5], Thermal and velocity slip effects on Casson nanofluid flow over an inclined permeable stretching cylinder via collocation method Usman et al [6],

Slip velocity and temperature jump of a non-Newtonian nanofluid, aqueous solution of carboxy-methyl cellulose/aluminum oxide nanoparticles, through a microtube Goodarzi et al [7], Thermal and velocity slip effects on MHD mixed convection flow of Williamson nanofluid along a vertical surface: modified Legendre wavelets approach Soomro et al [8], Slip flow of Maxwell viscoelasticity-based micropolar nanoparticles with porous medium: a numerical study Waqas et al [9], Review on Nano Enhanced PCMs: Insight on nePCM Application in Thermal Management/Storage Systems, Enery Mebarek et al [10], Effectiveness of induced magnetic force and non-uniform heat source/sink features for enhancing the thermal efficiency of third grade nanofluid containing microorganisms Khan et al [11], Thermal energy development in magnetohydrodynamic flow utilizing titanium dioxide, copper oxide and aluminum oxide nanoparticles: Thermal dispersion and heat generating formularization, Hafeez et al [12], Mathematical modeling and computational outcomes for the thermal oblique stagnation point investigation for non-uniform heat source and nonlinear chemical reactive flow of Maxwell nanofluid Abbasi et al [13], Forced convection three-dimensional Maxwell nanofluid flow due to bidirectional movement of sheet with zero mass flux Ahmad et al [14], Simultaneous features of Wu's slip, nonlinear thermal radiation and

activation energy in unsteady bio-convective flow of Maxwell nanofluid configured by a stretching cylinder Waqas et al [15], Peristaltic transportation of hybrid nano-blood through a ciliated micro-vessel subject to heat source and Lorentz force, Mebarek et al [16], Fluids of differential type: critical review and thermodynamic analysis Rajagopal et al[17], Boundary Layer Theory, Schichting et al[18], Rheology and Non-Newtonian Flow[19], Constitutive Equations for Polymer Melts and Solutions Larson et al[20]

2. MATHEMATICAL MODEL

Consider the two dimensional steady, viscous, incompressible, electrically non-conduccting boundary layer flow and heat transfer of biomagnetic fluid over a stretching sheet in the presence of magnetic dipole. Let the X-axis be taken along the direction of the sheet and Y axis be normal to it. Two equal and opposite forces are applied along the X-axis so that the sheet is stretched keeping the origin fixed. Assume that the sheet is stretched with velocity =cx, where c>0 is the stretching parameter. The temperature of the sheet is kept fixed and is free temperature which is situated far away from the sheet. The fluid is blood-based nanofluid containing Copper, Gold and Titanium dioxide nanoparticles. A magnetic dipole generated a magnetic field of strength which is located below the sheet at a distance d as depicted in Figure 1. Under these assumptions, the boundary layer equations governing the flow and heat field extending the idea of Sharma et al. [17] are portrayed in the following mathematical model

Figure 1

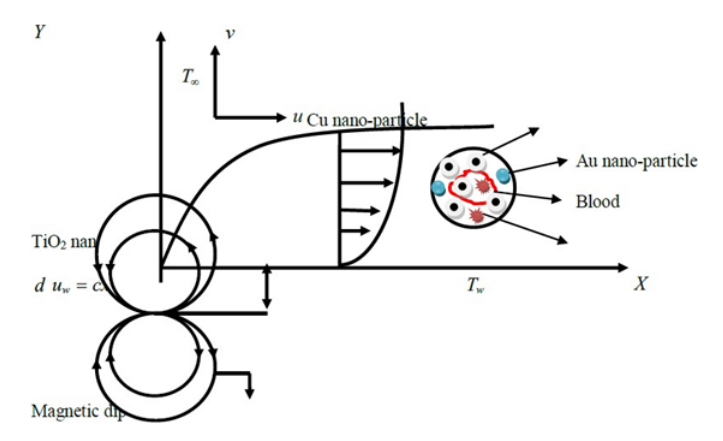


Figure 1 Geometry of the Problem

$$\frac{\partial \mathbf{u}}{\partial \mathbf{v}} + \frac{\partial \mathbf{v}}{\partial \mathbf{v}} = 0 \tag{1}$$

$$u\frac{\partial u}{\partial x} + v\frac{\partial u}{\partial y} = \frac{\mu_{\rm nf}}{\rho_{\rm nf}} \left(\frac{\partial^2 y}{\partial x^2}\right) + \frac{\mu_0}{\rho_{\rm nf}} M\frac{\partial H}{\partial x} + \lambda \left[u\frac{\partial^2 u}{\partial x^2} + v\frac{\partial^2 u}{\partial y^2} + 2uv\frac{\partial^2 u}{\partial x \partial y}\right]$$
(2)

$$u\frac{\partial T}{\partial x} + v\frac{\partial T}{\partial y} + \frac{\mu_0}{(\rho_{cp})_{nf}} T\frac{\partial M}{\partial T} \left(u\frac{\partial H}{\partial x} + v\frac{\partial H}{\partial y} \right) = \frac{k_{nf}}{(\rho_{cp})_{nf}} \left(\frac{\partial^2 T}{\partial y^2} \right)$$
(3)

With appropriate boundary conditions:

$$u = u_w + \frac{\partial u}{\partial y}, v = 0, T = T_w \quad \text{at } y = 0$$

$$u \to 0, \qquad T \to T_\infty \qquad \text{as} \quad y \to \infty$$

$$(4)$$

Where u and v are the velocity components of the nanofluid in the x and y-directions, respectively, T is the nanofluid tempature, T_{∞} is the free stream temperature, A is the velocity slip factor, M is the magnetization, H is the magnetic field of fluid, and μ_0 is the magnetic permeability.

Here μ_{nf} is the dynamic viscosity of the nanofluid, C_p is the specific heat at constant pressure, k_{nf} is the thermal conductivity of the nanofluid, and $\left(\rho_{cp}\right)_{nf}$ is the heat capacity at constant pressure of the nanofluid as defined in Sharma et al.

$$\mu_{\rm nf} = \mu_{\rm f} (1 - \emptyset)^{2.5}, \ (\rho_{\rm cp})_{\rm nf} = (1 - \emptyset)(\rho_{\rm cp})_{\rm f} + \emptyset(\rho_{\rm cp})_{\rm s}$$

$$\rho_{\rm nf} = (1 - \emptyset)\rho_{\rm s} + \emptyset\rho_{\rm s}$$

$$\frac{k_{nf}}{k_f} = \frac{(k_f + 2k_s) - 2\emptyset(k_f - k_s)}{(k_f + 2k_s) - \emptyset(k_f - k_s)}$$

Where \emptyset is the nanoparticle volume friction (\emptyset =0 corresponding to a regular fluid), ρ_f and ρ_s are the densities of the base fluid and the nanoparticle, respectively, k_f and k_s are the thermal conductivities of the base fluid and the nanoparticle, respectively, $\left(\rho_{cp}\right)_f$ and $\left(\rho_{cp}\right)_s$ are the heat capacitance of the base fluid and the nanoparticle, respectively.

The term $\mu_0 M \frac{\partial H}{\partial x}$ in equation (2) denotes the component of magnetic force per unit volume and depends on the presence of magnetic gradient. When the magnetic gradient is absent, this force vanishes. The second term, on the left-hand side of the thermal energy equation (3) accounts for accounts for heating due to adiabatic magnetization. The magnetic nanofluid is affected through the dipole field utilizing the magnetic scalar potential V such as,

$$V = \frac{\alpha}{2\pi} \frac{x}{x^2 + (y + d)^2}$$
, where α constant. (5)

The strength of magnetic field of the source position is represented by and denotes the distance from x-axis to the centre of magnetic field and the x, y components of magnetic field H are as follows:

$$H_x(x,y) = -\frac{\partial v}{\partial x} = \frac{\gamma}{2\pi} \frac{x^2 - (y+d)^2}{[x^2 - (y+d)^2]^2}$$

(6)

$$H_{y}(x,y) = -\frac{\partial v}{\partial y} = \frac{\gamma}{2\pi} \frac{2x(y+d)}{[x^{2} + (y+d)^{2}]^{2}}$$
(7)

Due to the force of the body being propotional to the gradient of magnitude H which is

$$H(x,y) = \left[H_x^2 + H_y^2\right]^{\frac{1}{2}} = \frac{\gamma}{2\pi} \left[\frac{1}{(y+d)^2} - \frac{x^2}{(y+d)^4}\right] \left[\frac{1}{(y+d)^2} - \frac{x^2}{(y+d)^4}\right]$$
(8)

By using equations (4) and (5) to solve equation (6) by expanding powers of and, we get

$$\frac{\partial H}{\partial x} = \frac{\gamma}{2\pi} \frac{-2x}{(y+d)^4}$$

$$\frac{\partial H}{\partial y} = \frac{\gamma}{2\pi} \left[\frac{-2}{(y+d)^3} + \frac{4x^2}{(y+d)^5} \right]$$

With the temperature T, the impact of magnetization M is expressed as

 $M = K(T - T_{\infty})$, where K shows pyromagnetic coefficient according to Andersson and Valnes

The continuity equation is automatically verified by presenting the subsequence of non-dimensional variables:

$$\eta = \sqrt{\frac{c}{\theta_f}} y, u = cxf'(\eta), v = \sqrt{c\theta_f} f(\eta), \theta(\eta) = \frac{T - T_{\infty}}{T_{w - T_{\infty}}}$$
(9)

where is the similarity variable and ϑ_f is the kinematic viscosity of the fluid.

After introducing (9) into (2) to (4), we obtain following ordinary differential equations:

$$f''' - (1 - \emptyset)^{2.5} \left(1 - \emptyset + \emptyset \frac{\rho_s}{\rho_f} \right) (f'^2 - ff'') - (1 - \emptyset)^{2.5} \frac{2\beta\theta}{(\eta + \alpha)^4} + \Gamma_1 (f^2 f'' + 2ff' f'') = 0, \tag{10}$$

$$\theta'' + \frac{\mathbf{p_r k_f} \left(\left(1 - \emptyset + \emptyset \frac{(\rho_{cp})_g}{(\rho_{cp})_f} \right) \right)}{\mathbf{k_{nf}}} f \theta' - \frac{2\lambda \beta f(\varepsilon + \theta) \mathbf{k_f}}{\mathbf{k_{nf}} (\eta + \alpha)^g} = 0$$
(11)

$$\theta'' + \frac{\frac{P_r k_f \left(\left(1 - \emptyset + \emptyset \frac{(\rho_{cp})_s}{(\rho_{cp})_f}\right)\right)}{k_{nf}} f \theta' - \frac{2\lambda \beta f(\epsilon + \theta) k_f}{k_{nf}(\eta + \alpha)^3} = 0$$

The boundary conditions are

$$f(0) = 0, f'(0) = 1 + \delta f''(0), \theta(0) = 1, f'(\infty) \to 0, \theta(\infty) \to 0,$$

$$f(0) = 0, f'(0) = 1 + \delta f''(0), \theta(0) = 1, f'(\infty) \to 0, \theta(\infty) \to 0,$$
(12)

Where prime (') denotes the differentiation with respect to η .

$$Pr = \frac{\vartheta_f(\left(\rho_{cp}\right)_f}{k_f} \text{ is the Prandtl number, } \lambda = \frac{c\mu_f^2}{\rho_{fk_f}(T_w - T_\infty)} \text{ is the viscous dissipation parameter,}$$

$$\beta = \frac{\gamma}{2\pi} \frac{\mu_0 K \rho_{f(T_W - T_\infty)}}{\mu_f^2} \qquad \text{is the ferromagnetic interaction parameter, } \epsilon = \frac{T_\infty}{T_W - T_\infty} \text{is the dimensionless Curie}$$

temperature, $\alpha = \sqrt{\frac{c}{\vartheta_f}} \, dis$ the dimensionless distance,

$$Re = \frac{xu_w}{\theta_f} \text{is the local Reynolds number and } \delta = A \sqrt{\frac{c}{\theta_f}} \quad \text{is the slip parameter, } \Gamma_{1=\lambda c} \text{ is the max well parameter.}$$

The most important physical measurements are the skin friction coefficients and Nusselt number. The explanation of this dimensionless physical measurement is given as

$$-C_{f} = \frac{\mu_{nf}}{\rho_{f} u_{w}^{2}} \left(\frac{\partial u}{\partial y}\right)_{v=0} \tag{13}$$

$$Nu = -\frac{k_{nf}}{k_f(T_w - T_\infty)} \left(\frac{\partial T}{\partial y}\right)_{y=0} \tag{14}$$

With the help of similarity variables, equations (13) and (14) reduce to

$$R_{e}^{\frac{1}{2}}C_{f} = \frac{1}{(1-\phi)^{2.5}}f''(0)$$
And
$$R_{e}^{\frac{-1}{2}}Nu = -\frac{k_{nf}}{k_{f}}\theta'(0)$$
(15)

3. NUMERICAL METHOD

 $f' = y_2$

Now we solve the set of nonlinear ordinary differential equation (10) and (11) with the boundary conditions (12) numerically by using bvp4c function technique Maple package. We consider, $f = y_1$, $f' = y_2$, $f'' = y_3$, $\theta = y_4$, $\theta' = y_5$. Then the equations and boundary condition are transformed into a system of first ordinary differential equation as given below:

$$f'' = y_2' = y_3$$

$$f''' = y_3' = (1 - \emptyset)^{2.5} \left(1 - \emptyset + \emptyset \frac{\rho_s}{\rho_f} \right) (y_2^2 - y_1 y_3) + (1 - \emptyset)^{2.5} \frac{2\beta y_4}{(\eta + \alpha)^4}$$

$$\theta' = y_5$$

$$(k_f + 2k_c) + \emptyset (k_f - k_c) \left[(\rho_{CD})_c \right] \qquad (k_f + 2k_c) + \emptyset (k_f - k_c) 2\beta \lambda y_1 (\varepsilon + \theta)$$

$$\theta'' = y_5' = \frac{(k_f + 2k_s) + \emptyset(k_f - k_s)}{(k_f + 2k_s) - 2\emptyset(k_f - k_s)} Pr \left[1 - \emptyset + \emptyset \frac{(\rho_{cp})_s}{(\rho_{cp})_f} \right] y_1 y_5 + \frac{(k_f + 2k_s) + \emptyset(k_f - k_s)}{(k_f + 2k_s) - 2\emptyset(k_f - k_s)} \frac{2\beta \lambda y_1(\epsilon + \theta)}{(\eta + \alpha)^3}$$

Along with the initial boundary conditions:

$$y_2(0) = 1 + \delta y_3(0), y_1(0) = 0, y_4(0) = 1, y_2(\infty) = 0,$$
 (17)

Equations (16) and (17) are integrated numerically as an initial value problem to a given terminal point. All these simplifications are made by using byp4c function available in MAPLE software.

4. CAMPARISON WITH PREVIOUS WORK AND VALUES OF THERMO-PHYSICAL PROPERTIES

For the accuracy and validity, we compared the present numerical values to the Nusselt number with that of various values of volume friction \emptyset and Pradtl number Pr with β =0. The comparision shows an excellent agreement as shown im Table 1.

Table 1. Comparison values of - (0) for different values of and Pr

Ø	Pr	Sharma et al. [17]	Present results
0	3	1.165101358	1.164063
	10	2.307564425	2.101522
0.1	6.2	1.474327348	1.474779
0.2	_	1.245900088	1.244917

Table 2. Thermophysical properties of blood and nanoparticle

Thermophysical Properties	Base fluid		Nano particles	
	Blood	Cu	TiO ₂	Au
c _p (J/kg K)	3594	385	686.2	129

ρ(Kg/m ³)	1063	8933	4250	19300	-
k(W/mK)	0.492	401	8.9538	318	

5. RESULTS AND DISCUSSION

This segment deliberates the details about the consequences of the problems that are drawn using the numerical method. the impacts of various emerging flow variables on blood with Copper, Gold and Titanium dioxide nanoparticles are described via graphical illustration of velocity, temperature, skin friction coefficient and heat transfer rate. For numerical solution, it is essential to take some numerical values for the parameters concerned in the study under investigation. A factual case is treated in which the fluid is blood, temperature of curie number and the viscous dissipation number as started by Alam and Murtaza[21].

We utilize the following parameters in figure 2-15:

- 1) Prandtl number Pr=17,21,25 as in Alam and Murtaza [21].
- 2) Ferromagnetic number $\beta = 0$ to 10 as in (Alam and Murtaza [21]).
- 3) Note that β =0 corresponds to hydrodynamic flow.
- 4) Volume friction $\emptyset = 0.05, 0.1, 0.2$ as in Sharma et al. [17].
- 5) Dimensionless distance $\propto =1$ as in Alam and Murtaza [21].
- 6) Velocity slip parameter δ =0.1,0.2,0.3 as in Sharma et al [17].

Figures 2 depict the velocity and temperature profiles for various values of slip parameter. From the figures, it is observed that velocity profile increases and temperature profiles decreases with increasing values of slip parameter in all the cases, whereas temperature profile increases in all the cases. In thermal boundary layer, Au-blood is higher compared than Cu-blood and TiO2-blood.

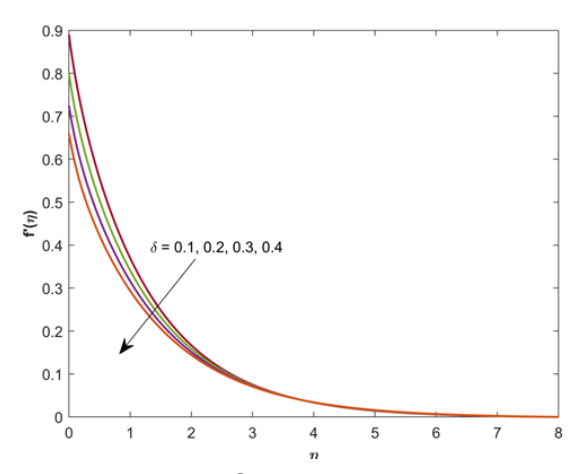


Figure 2. Velocity Profile for $f'(\eta)$ for various values of δ

Figure 3 and 4 depict the velocity and temperature profiles for various values of ferromagnetic number (β). From the figures, it is observed that velocity profile decreases and temperature profiles increases with increasing values of ferromagnetic parameter in the case. The presence of ferrite nanoparticles in the fluid causes an increase in the thickness of the fluid, as a result reduction in the velocity field when β is increased.

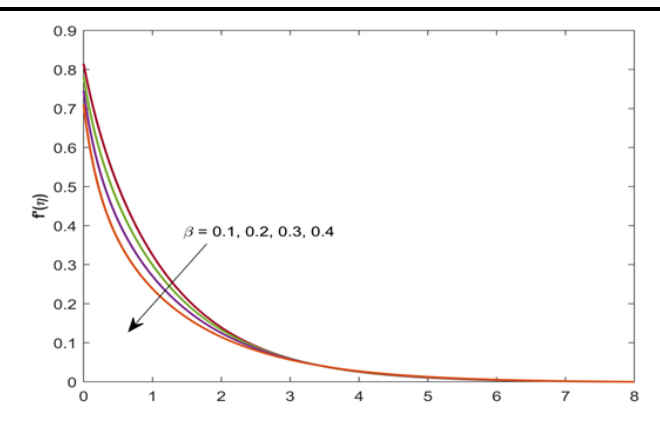


Figure 3. Velocity profile for $f'(\eta)$ for various values of β

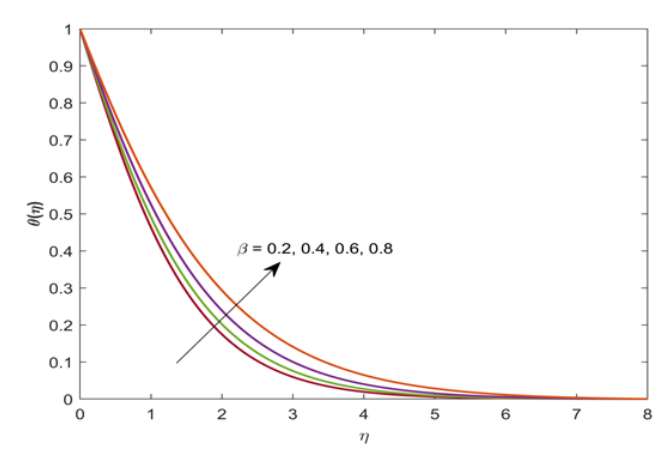


Figure 4. Temperature Profile for $\theta(\eta)$ for various values of β

Figure 5 and 6 depict the velocity and temperature profiles for various values of dimensionless distance (α). From the figure, it is observed that velocity profile increases and temperature profile decreases with increasing values of dimensionless distance in all the cases. The velocity profile of the fluid increases with the dimensionless distance from the boundary, reflecting a transition from slower velocities near the surface to higher velocities farther from it.

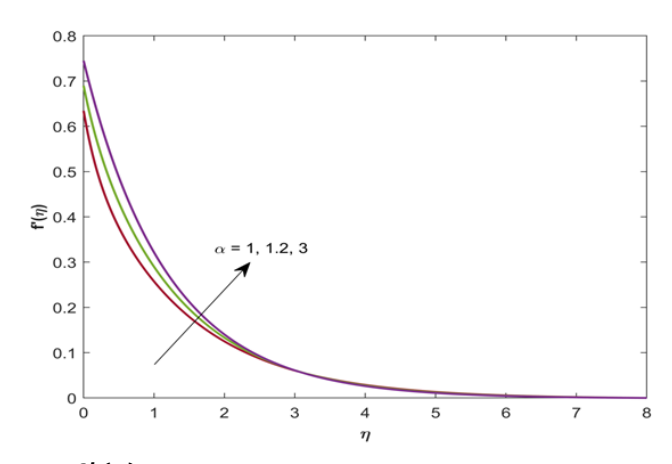


Figure 5. Velocity Profile for $f'(\eta)$ for various values of α .

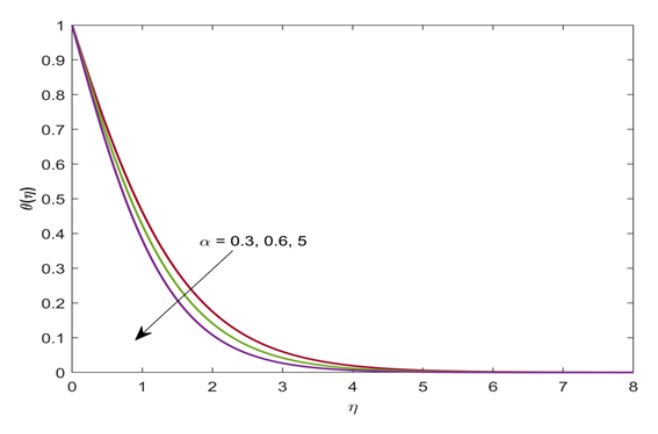


Figure 6. Temperature profile for $\theta(\eta)$ for various values of α .

Figure 7 show the temperature profile for the various values of dimensionless Curie temperature (ε). It is noticed that temperature profile decreases if the dimensionless Curie temperature decreases, it means that the Curie temperature, when expressed relative to a reference temperature, is falling. In practical terms, this implies that the temperature at which a material loses its ferromagnetic properties is dropping.

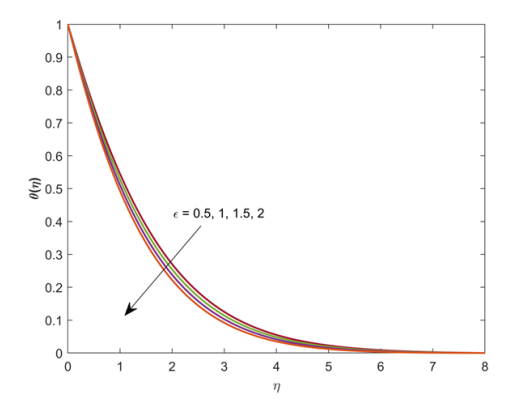


Figure 7. Temperature profile for $\theta(\eta)$ for various values of ϵ .

Figure 8 show the temperature profile for the various value of viscous dissipation parameter (λ). It is noticed the viscous dissipation parameter measures the effect of viscous forces on energy dissipation with in fluid. A decreases in this parameter indicates that the fluid experiences less energy loss due to viscosity. A decrease in the viscous dissipation parameter leads to a reduction in the temperature of the fluid because less energy is being converted into heat through viscous effects.

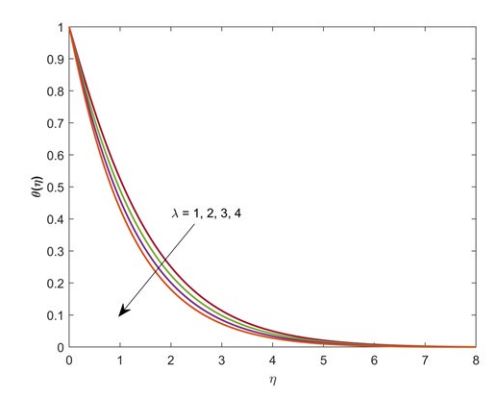


Figure 8. Temperature profile for $\theta(\eta)$ for various values of λ .

Figure 9 shows the velocity profile for various values of Maxwell parameter (Γ_1). It is noticed that velocity profile increases if the Maxwell parameter increases, the Maxwell parameter is related to the elasticity and viscosity of a fluid.

When the Maxwell parameter increases, it generally indicates a higher elasticity or a more significant viscoelastic response of the fluid. This increased elasticity can lead to a change in the fluid's velocity profile. Specifically, a higher Maxwell parameter often means that the fluid exhibits greater resistance to deformation, which can alter how quickly different layers of the fluid move relative to each other. As a result, the velocity profile of the fluid becomes more pronounced, with steeper gradients between different flow regions. This change is due to the fluid's increased ability to store and return elastic energy, which influences the distribution and magnitude of the velocity throughout the flow. Consequently, the overall flow behavior becomes more complex, and the velocity profile reflects these changes by becoming more sensitive to variations in the applied forces and flow conditions.

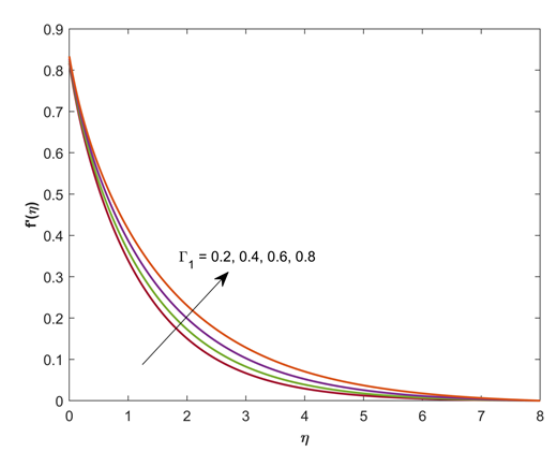


Figure 9. Velocity profile for $f'(\eta)$ for various values of

6. CONCLUSIONS

We have studied the biomagnetic flow and heat transfer of an incompressible, electrically nonconducting blood based, Copper, Gold and Titanium dioxide nanoparticles past over a stretching sheet in the presence of magnetic dipole by considering slip condition. The major conclusions of this work are as follows:

- 1) The velocity profile decreases with the increasing the value of slip parameter.
- 2) The velocity profile decreases with the increasing the value of ferromagnetic interaction parameter.
- 3) The Temperature profile increases with the increasing the value of ferromagnetic interaction parameter.
- 4) The velocity profile increases with the increasing the value of dimensionless distance.
- 5) The Temperature profile decreases with the increasing the value of dimensionless distance
- 6) The Temperature profile decreases with the increasing the value of dimensionless Curie temperature.
- 7) The velocity profile increases with the increasing the value of Maxwell parameter.
- 8) The Temperature profile decreases with the increasing the value of viscous dissipation parameter.

CONFLICT OF INTERESTS

None.

ACKNOWLEDGMENTS

None.

REFERENCES

Haik Y, Pai V and Chen C J.,1999. Biomagnetic fluid dynamics, in fluid dynamics at interfaces. edited by W. Shyy and R. Narayanan (Cambridge University Press, Cambridge), 439-452. 2

- Manjunatha, S., Gireesha, B.J., 2016. Effects of variable viscosity and thermalconductivity on MHD flow and heat transferof a dusty fluid, Ain Shams Engineering Joutrnal,7(1), 505-515. 21
- Sajid M, Abbas Z, Ali N, Javed T, Ahmad I.2014. Slip flow of a Maxwell fluid past a stretching sheet. Walailak Journal of Science and Technology. 11(12), 1093-1103
- R. Naveen Kumar, A.M. Jyothi, Hesham Alhumade, R.J. Punith Gowda, Mohammad Mahtab Alam, Irfan Ahmad, M.R. Gorji, B.C. Prasannakumara, 2021. Impact of magnetic dipole on thermophoretic particle deposition in the flow of Maxwell fluid over a stretching sheet, Journal of Molecular Liquids, 334, 116494. 15
- MOUSAVI, S. M., DARZI, A. A. R., AKBARI, O. A., TOGHRAIE, D., and MARZBAN, A. Numerical study of biomagnetic fluid flow in a duct with a constriction affected by a magnetic field. Journal of Magnetism and Magnetic Materials, 473, 42–50 (2019)
- USMAN, M., SOOMRO, F. A., HAQ, R. U., WANG, W., and DEFTERLI, O. Thermal and velocity slip effects on Casson nanofluid flow over an inclined permeable stretching cylinder via collocation method. International Journal of Heat and Mass Transfer, 122, 1255–1263 (2018)
- GOODARZI, M., JAVID, S., SAJADIFAR, A., NOJOOMIZADEH, M., and MOTAHARIPOUR, S. H. Slip velocity and temperature jump of a non-Newtonian nanofluid, aqueous solution of carboxy-methyl cellulose/aluminum oxide nanoparticles, through a microtube. International Journal of Numerical Methods for Heat and Fluid Flow, 29(5), 1606–1628 (2019)
- SOOMRO, F. A., USMAN, M., HAQ, R. U., and WANG, W. Thermal and velocity slip effects on MHD mixed convection flow of Williamson nanofluid along a vertical surface: modified Legendre wavelets approach. Physica E: Low-dimensional Systems and Nanostructures, 104, 130–137 (2018)
- WAQAS, H., IMRAN, M., KHAN, S. U., SHEHZAD, S. A., and MERAJ, M. A. Slip flow of Maxwell viscoelasticity-based micropolar nanoparticles with porous medium: a numerical study. Applied Mathematics and Mechanics (English Edition), 40(9), 1255–1268 (2019) https://doi.org/10.1007/s10483-019-2518-9
- F. Mebarek-Oudina, I. Chabani, Review on Nano Enhanced PCMs: Insight on nePCM Application in Thermal Management/Storage Systems, Energies 16 (2023) 1066, https://doi.org/10.3390/en16031066
- N. Khan, et al., Maxwell nanofluid fow over an infinite vertical plate with ramped and isothermal wall temperature and concentration, Math. Probl. Eng. (2021), https://doi.org/10.1155/2021/3536773.
- M.B. Hafeez, M. Krawczuk, W. Jamshed, El S.M. Tag El Din, H.A.W. El Khalifa, F. A. Seabee, Thermal energy development in magnetohydrodynamic flow utilizing titanium dioxide, copper oxide and aluminum oxide nanoparticles: Thermal dispersion and heat generating formularization, Front. Energy Res. 10 (2022) 1000796, https://doi.org/10.3389/fenrg.2022.1000796.
- Y.-M. Chu, A. Abbasi, K. Al-Khaled, W. Farooq, S.U. Khan, M.I. Khan, S.M. Eldin, K. Guedri, Mathematical modeling and computational outcomes for the thermal oblique stagnation point investigation for non-uniform heat source and nonlinear chemical reactive flow of Maxwell nanofluid, Case Studies in Thermal Engineering 41 (2023), 102626, https://doi.org/10.1016/j.csite.2022.102626.
- M. Ahmad, E. Rashdy, K. Al-Khaled, M. Rasheed, S.U. Khan, M. Taj, M.I. Khan, S. Elattar, Forced convection three-dimensional Maxwell nanofluid flow due to bidirectional movement of sheet with zero mass flux, Int. Commun. Heat Mass Transfer 135 (2022), 106050, https://doi.org/10.1016/j.icheatmasstransfer.2022.106050.
- Y.-X. Li, H. Waqas, K. Al-Khaled, S.A. Khan, M.I. Khan, S.U. Khan, R. Naseem, Y.- M. Chu, Simultaneous features of Wu's slip, nonlinear thermal radiation and
- activation energy in unsteady bio-convective flow of Maxwell nanofluid configured by a stretching cylinder, Chin. J. Phys. 73 (2021) 462–478, https://doi.org/10.1016/j.cjph.2021.07.033.
- Ali, F. Mebarek-Oudina, A. Barman, S. Das, A.I. Ismail, Peristaltic transportation of hybrid nano-blood through a ciliated micro-vessel subject to heat source and Lorentz force, J. Therm. Anal. Calorim. 148 (2023) 7059–7083, https://doi.org/10.1007/s10973-023-12217.
- H. Schichting, Boundary Layer Theory, sixth ed., McGrawHill, New York, 1964.
- J. Harris, Rheology and Non-Newtonian Flow, Longman, London, 1977.
- R.G. Larson, Constitutive Equations for Polymer Melts and Solutions, Butterworths, Boston, 1988.